INFECTION AND IMMUNITY, July 2005, p. 3878–3887 Vol. 73, No. 7
0019-9567/05/$08.00+0 doi:10.1128/IAI.73.7.3878–3887.2005

Noninvasive Biophotonic Imaging for Monitoring of Catheter-Associated Urinary Tract Infections and Therapy in Mice

Jagath L. Kadurugamuwa,* Kshitij Modi, Jun Yu, Kevin P. Francis, Tony Purchio, and Pamela R. Contag

Xenogen Corporation, 860 Atlantic Avenue, Alameda, California 94501

Received 12 November 2004/Returned for modification 16 February 2005/Accepted 9 March 2005

Urinary tract infections (UTIs) are among the most common bacterial infections acquired by humans, particularly in catheterized patients. A major problem with catheterization is the formation of bacterial biofilms on catheter material and the risk of developing persistent UTIs that are difficult to monitor and eradicate. To better understand the course of UTIs and allow more accurate studies of in vivo antibiotic efficacy, we developed a catheter-based biofilm infection model with mice, using bioluminescently engineered bacteria. Two important urinary tract pathogens, *Pseudomonas aeruginosa* and *Proteus mirabilis*, were made bioluminescent by stable insertion of a complete *lux* operon. Segments of catheter material (precolonized or postimplant infected) with either pathogen were placed transurethrally in the lumen of the bladder by using a metal stylet without surgical manipulation. The bioluminescent strains were sufficiently bright to be readily monitored from the outside of infected animals, using a low-light optical imaging system, including the ability to trace the ascending pattern of light-emitting bacteria through ureters to the kidneys. Placement of the catheter in the bladder not only resulted in the development of strong cystitis that persisted significantly longer than in mice challenged with bacterial suspensions alone but also required prolonged antibiotic treatment to reduce the level of infection. Treatment of infected mice for 4 days with ciprofloxacin at 30 mg/kg of body weight twice a day cured cystitis and renal infection in noncatheterized mice. Similarly, ciprofloxacin reduced the bacterial burden to undetectable levels in catheterized mice but did not inhibit rebound of the infection upon cessation of antibiotic therapy. This methodology easily allows spatial information to be monitored sequentially throughout the entire disease process, including ascending UTI, treatment efficacy, and relapse, all without exogenous sampling, which is not possible with conventional methods.

Urinary tract infections (UTI) are one of the most common bacterial infections in humans (9, 35). The majority of these infections follow instrumentation of the urinary tract, mainly urinary catheterization, with the development of catheter-associated bacteriuria being directly related to the duration of implant (6, 18, 37, 44). Thus, it is commonplace for the incidence of bacteriuria to be as high as 95% in catheterized patients with implants present for 30 days or more (6, 44). Complications with such infections can lead to fever, cystitis, acute pyelonephritis, bacteremia, and death (44). Catheter-associated urinary tract infections are caused by a variety of uropathogens, including *Escherichia coli*, *Klebsiella*, *Proteus*, *Enterococcus*, *Pseudomonas*, *Enterobacter*, *Serratia*, and *Candida* (6, 44).

Typically, the bacterial biofilm growth on urinary catheter and adjacent mucosa accounts for the pathophysiology of catheter-associated UTI (25, 26, 31). Diseases involving bacterial biofilms are generally chronic and difficult to treat, because bacteria in the biofilm mode of growth are more resistant to antimicrobial agents than their planktonic counterparts (5, 21, 29). Most often, catheter infections require removal of the device before a cure is achieved (6, 32). In order to prevent and treat these catheter-associated infections, new approaches to screen candidate therapeutic agents, especially in vivo, are needed to accelerate their development.

* Corresponding author. Mailing address: Xenogen Corporation, 860 Atlantic Avenue, Alameda, CA 94501. Phone: (510) 291 6246. Fax: (510) 291 6196. E-mail: jagath.kadurugamuwa@xenogen.com.

To this end, recent advances in biophotonic imaging technology together with bioluminescent reporters provide a sensitive and simple detection method for the study of biological processes in live animal models of human biology and disease. The use of luciferase to tag pathogens has proved to be a valuable tool to provide an in vivo tracking system. Light-emitting bacteria and virus can be detected within the animal by noninvasive optical biophotonic imaging (3, 4, 7, 10, 15, 20, 24, 30, 47, 48). Recently we demonstrated the application of this technology to study chronic soft-tissue biofilm infections and the therapeutic efficacy of several antibiotics in a mouse model (20–22). This technique has also been demonstrated to work particularly well for monitoring catheter-associated endovascular infections, such as endocarditis, in rats and mice (42, 45). Here, we developed an animal model of catheter-associated UTI for direct visualization of infection from outside intact live animals. In vivo bioluminescence imaging was employed to determine the initial location of the infection and the spatial migration of two important bioluminescently engineered uropathogens, *Pseudomonas aeruginosa* and *Proteus mirabilis*, over time in live animals. Using this approach, we were able to follow the processes of infection over a period of days in diseased animals as well as animals with no clinical signs. In addition, we demonstrated the utility of the model in assessing the in vivo efficacy of antibiotic therapy for UTI in real time in living animals.

(Parts of the present study were presented at the 104th

General Meeting of the American Society for Microbiology [28], New Orleans, La., 2004).

MATERIALS AND METHODS

Bacterial strains. The bacterial strains used in this study were *Pseudomonas aeruginosa* ATCC 19660 (20) and *Proteus mirabilis* ATCC 51286. These strains were engineered for bioluminescence by inserting a *Photorhabdus luminescence luxCDABE* operon as described previously and subsequently designated *P. aeruginosa* Xen 5 (20) and *P. mirabilis* Xen 44.

Generation of bioluminescent *P. mirabilis*. *P. mirabilis* strain ATCC 51286 (a clinical isolate from a patient suffering from a urinary catheter infection) was made bioluminescent by the random insertion of a transposon, mini-Tn*5* *luxCDABE kan*^{r}, into the chromosome. A highly bioluminescent colony was selected from the transposon recipients, identified, and designated *P. mirabilis* Xen 44. Chromosomal DNA of bioluminescent *P. mirabilis* Xen 44 was digested with the restriction enzyme SspI and then self ligated. The ligated fragment served as a template for inverse PCR amplification using *Pfu* DNA polymerase (Stratagene, La Jolla, CA) and the primers UTCF1 (5′GTG CAA TCC ATT AAT TTT GGT G 3′) and UTCR (5′ CAT ACG TAT CCT CCA AGC C 3′) to amplify the region upstream of the transposon insertion site. The resulting PCR fragments were purified using a PCR purification kit and sequenced with UTCF1 and UTCR as primers. The sequencing results were BLAST searched against the National Center for Biotechnology Information database.

Catheter-associated biofilms. Biofilms of *P. aeruginosa* and *P. mirabilis* were allowed to grow on PE50 (outside diameter, 0.965 mm; inside diameter, 0.58 mm) catheter material (Braintree Scientific) as described previously (20). This catheter material is routinely used clinically.

Antibiotic susceptibility testing. (i) MIC assays. MICs were determined by the broth dilution method using an inoculum of 10^6 CFU/ml *P. aeruginosa* or *P. mirabilis* in Müeller-Hinton broth (MHB) by the procedures recommended by the National Committee for Clinical Laboratory Standards as described previously (21).

(ii) Biofilm susceptibility testing. The biofilms that formed on 6-mm catheter segments were transferred to tubes containing dilutions of the antibiotic in MHB. Following 18 h of incubation at 37°C in the presence of this antimicrobial agent, the catheters were rinsed twice in MHB, and the viability and metabolic activity of the biofilm were determined by measurement of viable counts and reading the bioluminescence using an IVIS imaging system (100 series) (Xenogen Corp., Alameda, CA), as described previously (21). The minimal biofilm eradication concentration was defined as the lowest concentration of antibiotic that reduced ≥99.9% of the biofilm cell numbers after 24 h of incubation at 37°C, with respect to the cell numbers for the untreated controls.

Experimental mouse model of UTI. The experimental catheter-associated UTI in a rat model developed by Kurosaka et al. (26) was established in mice with the following modifications. All experimental procedures for the animals were performed in accordance with guidelines of the Institutional Animal Care and Use Committee. Six-millimeter-long segments (outside diameter, 0.965 mm; inside diameter, 0.58 mm) of polyethylene tube (PE50 Braintree Scientific, Inc.) were fitted onto a flexible metal wire, spiraled around a similar metal wire, and placed in boiling water for 1 min. The tubing was removed, and each piece was sterilized with 70% ethanol and air dried. Bacterial biofilms were grown on the tubing as described previously (20). The metal stylet of a 24-gauge Teflon catheter (Abbocath-T; Burns Vet Supply, Vancouver, WA) that has been cut to approximately 5 cm was then fitted with polyethylene tubing that had been colonized with bacteria or a segment of sterile tubing. CF-1 female mice (Charles River, Wilmington, Mass) weighing 26 to 30 g were maintained in an anesthetized state with 2.5% isoflurane gas and placed on their backs. After cleansing of the periurethral area with 70% ethanol, the papilla was grasped with light pressure using forceps and lifted away from the abdomen. While the papilla was maintained in this position, the end of the stylet bearing the 6-mm-long tubing was advanced into the urethral opening until the leading end was in the bladder. The Teflon catheter was advanced until the shorter segment was pushed off the stylet, thereby leaving the 6-mm-long polyethylene catheter tubing free in the bladder lumen. Subsequently, the stylet with the Teflon catheter was removed. The 6-mm-long catheter tubing in the bladder reverted spontaneously to its spiral shape and remained in place until the end of the monitoring period. Infection was induced by either implanting a precolonized catheter segment carrying a defined inoculum or by implanting a segment of sterile catheter in the bladder and inoculating the bladder immediately with defined quantities of pathogen in 50 μl phosphate-buffered saline (PBS) over 30 s by insertion of the Teflon catheter into the bladder through the urethra. The Teflon catheter was removed immediately after inoculation. Previous studies have shown that this procedure does not induce vesicoureteral reflux of the inoculum (14, 18, 23). In some studies the UTI was induced in uncatheterized mice by transurethral inoculation of defined quantities of bacterial suspension in 50 μl of PBS directly into the bladder via urethral catheter. The inoculating doses were prepared as described previously (20). The doses for *P. aeruginosa* Xen 5 and *P. mirabilis* Xen 44 were 1.6×10^6 CFU/catheter or 2.0×10^6 CFU/50-μl suspensions and 7.1×10^3 CFU/catheter or 1.3×10^4 CFU/50-μl suspensions, respectively (20). Inoculum studies indicated the above challenge doses produced optimal success in generating chronic UTIs.

Antimicrobial therapy. Ciprofloxacin (USP, Rockville, MD), which has been shown to have unique activity against UTI infections due to gram-negative uropathogens, was selected for treatment (38, 43, 46). Treatment of animals with catheter-associated infection commenced 2 days after bacterial challenge with a dose of 30 mg/kg of body weight ciprofloxacin given orally in 0.2 ml of water twice daily for four consecutive days. This dose of ciprofloxacin was previously shown to have bactericidal effect against several uropathogens in mouse models of experimental UTI (13, 39, 46). A second group of animals served as an untreated infection control group by being implanted with infected catheters and treated with saline. In another control group, animals were implanted with sterile catheters and served as a negative control. The antibiotic was readministered for four consecutive days to a group of animals with reestablished infection after 3 days of cessation of the initial therapy.

Bacteriological examination. At the indicated times, the urine was pressed out from the animal by gentle compression of the bladder through the abdominal wall. Samples of urine were collected from the external urethral meatus by using a micropipette. Bacterial titers in urine were determined by plating serial dilutions on tryptic soy broth or MacConkey agar plates. The lower limits of detection of bacteria by bioluminescence and conventional methods in mouse bladder and urine for *P. aeruginosa* Xen 5 and *P. mirabilis* Xen 44 were $<10^3$ and $<10^2$ CFU/ml, respectively.

Imaging procedure. Prior to imaging, mice were anesthetized with 2 to 2.5% isoflurane gas, and the entire animal was imaged for a maximum of 5 min at various times following catheter implantation and treatment using an IVIS imaging system (100 series) (Xenogen Corp., Alameda, CA). During the imaging, mice were maintained in an anesthetized state with 2.5% isoflurane, using an IVIS manifold placed inside the imaging chamber. Total photon emissions from defined regions of interest within the images of each mouse were quantified using the Living Image software (Xenogen Corporation, Alameda, CA) as described previously (20). The photon signals were quantified from the dorsal and ventral images of each mouse. During the treatment, and after the final imaging time point, mice were euthanized; the kidneys and infected catheters were harvested. Organ homogenates and bacteria detached from catheters were enumerated by both bioluminescence imaging and the conventional viable count method as described previously (20). Bacteria recovered at the end of the experimental period were analyzed with the inoculating strain for comparative bioluminescence to ensure stability of the *lux* construct during the procedure.

Scanning electron microcopy. Catheter segments were washed with PBS and placed in 2.5% glutaraldehyde fixative overnight at room temperature and prepared for Scanning electron microcopy at Southern Illinois University (Integrated Microscopy and Graphics Expertise, Carbondale, IL).

RESULTS

Characterization of *P. mirabilis* Xen 44. The chromosomal integration site of the *P. mirabilis* Xen 44 construct determined by inverse PCR indicated that the transposon had inserted at position 397 of a 460-amino-acid putative mating-pair formation protein, TrbI, which is involved in the conjugal transfer of plasmid DNA. The growth characteristics of parental *P. mirabilis* and its bioluminescent derivative, *P. mirabilis* Xen 44, were compared and found to be identical.

Antimicrobial susceptibility studies. The MICs of ciprofloxacin for *P. aeruginosa* Xen 5 and *P. mirabilis* Xen 44 were 0.125 and 0.03 μg/ml, respectively. The corresponding minimal biofilm eradication concentrations were 4 and 1 μg/ml, respectively.

Biophotonic monitoring of UTI due to *P. aeruginosa* Xen 5 and *P. mirabilis* Xen 44 in mice. Bioluminescence monitoring of the course of infection following inoculation of mice transurethrally either with bacterial suspensions or by placement of a segment of precolonized catheter with *P. aeruginosa* Xen 5 or *P. mirabilis* Xen 44 is shown in Fig. 1A and B, respectively. The

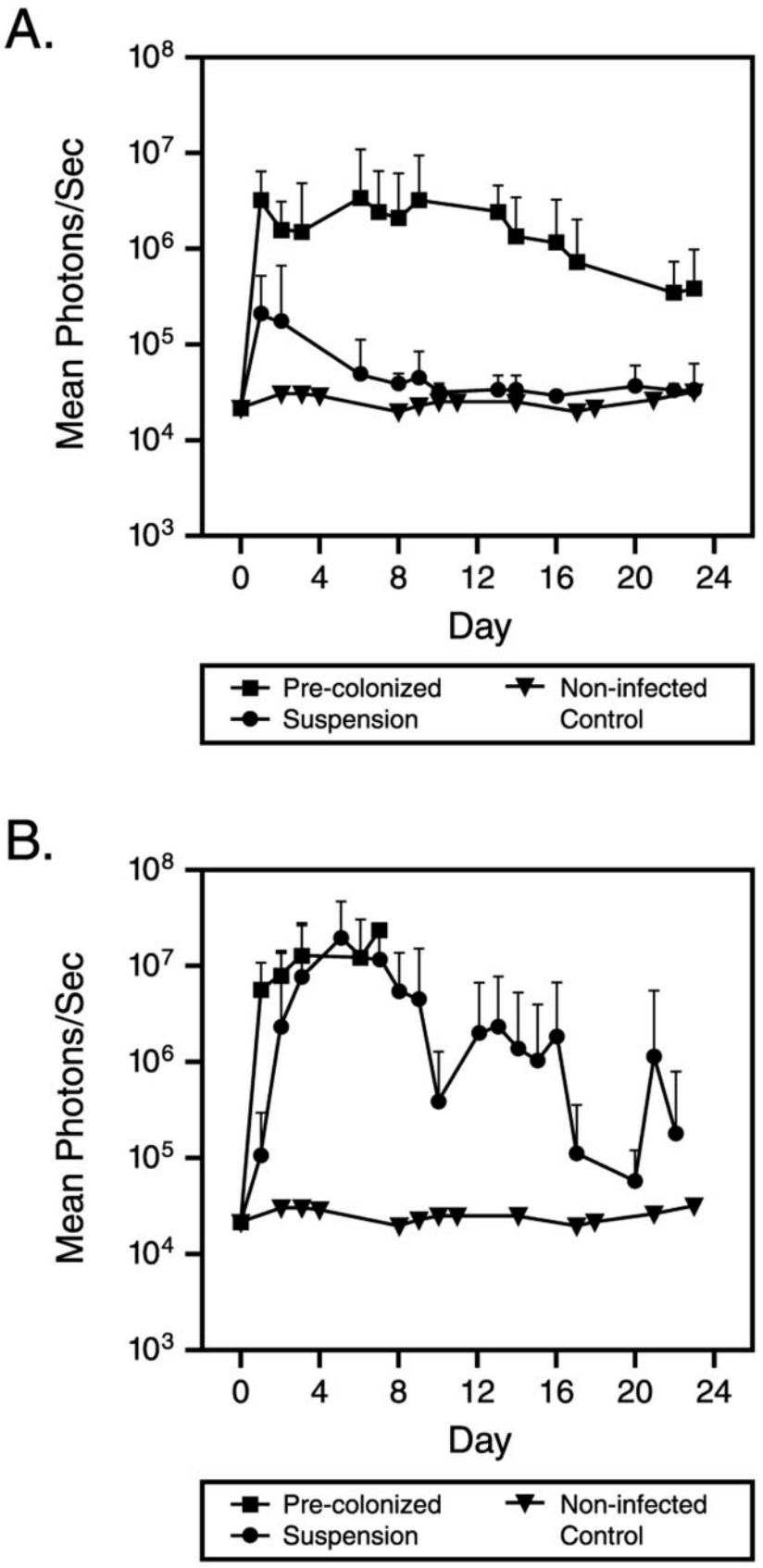

FIG. 1. (A and B) Growth and bioluminescence curves of (A) *P. aeruginosa* Xen 5 and (B) *P. mirabilis* Xen 44 UTI in mice infected with precolonized catheters or bacterial suspensions. UTI was induced by implanting a precolonized catheter in the bladder or by transurethral inoculation of the bladder with a bacterial suspension. The total photon emissions from the infected sites were quantified using Living Image software (cumulative results are shown). Each data point is the mean ± standard error for 13 to 19 mice. Results for postimplant infection were similar to those for precolonized infection except that the bioluminescence signal peaked 2 days after infection.

TABLE 1. Mortality and infection rate in mice infected with *P. aeruginosa* Xen 5 and *P. mirabilis* Xen 44

Mode of infection	Day after infection	% Mortality		No. of animals with bladder infection/total no. (%[a])		No. of animals with kidney infection/total no. (%[a])	
		XEN5	XEN44	XEN5	XEN44	XEN5	XEN44
Suspension	1	0	0	6/14 (43)	3/15 (20)	0/14 (0)	1/15 (7)
	2	0	0	2/14 (14)	5/15 (33)	0/14 (0)	1/15 (7)
	7	0	0	1/14 (7)	8/15 (53)	0/14 (0)	4/15 (27)
	9	0	7	1/14 (7)	5/14 (36)	0/14 (0)	3/14 (21)
	15	0	7	0/14 (0)	4/14 (29)	0/14 (0)	3/14 (21)
Postimplant infection	1	8	8	10/11 (91)	9/11 (82)	2/11 (18)	2/11 (18)
	2	17	8	8/10 (80)	9/11 (82)	2/10 (20)	6/11 (55)
	7	33	75	7/8 (88)	0/3 (0)	2/8 (25)	0/3 (0)
	9	42	75	5/7 (71)	0/3 (0)	1/7 (14)	0/3 (0)
	15	42	75	7/7 (100)	0/3 (0)	1/7 (14)	0/3 (0)
Precolonized infection	1	0	0	17/19 (90)	13/13 (100)	1/19 (5)	0/13 (0)
	2	0	0	16/19 (84)	13/13 (100)	2/19 (11)	5/13 (39)
	7	21	92	12/15 (80)	1/1 (100)	4/15 (27)	1/1 (100)
	9	32	100	11/13 (85)		2/13 (15)	
	15	42	100	10/11 (91)		4/11 (36)	

[a] % Animals with infection.

infection of animals due to different modes of inoculations is summarized in Table 1. At day 1 postinfection, the bladder signal increased to 10^5 photons/s in mice inoculated with a bacterial suspension of *P. aeruginosa* Xen 5 (Fig. 1A). The signal intensity declined steadily thereafter to undetectable levels by day 10, thus indicating spontaneous clearance of the infection from these animals. The bladder signals in mice inoculated with a suspension of *P. mirabilis* Xen 44 were higher than those with *P. aeruginosa* Xen 5 and reached levels of 10^7 photons/s by day 3. Thereafter, the signal began to decrease, disappearing completely from some animals only to reappear at various times later, indicating the transitory nature of this infection (Fig. 1B and Table 1). These fluctuations in bioluminescence from the bladder correlated with bacterial counts in urine from these animals (Table 2). We observed a strong correlation between the intensity of bladder bioluminescence and the viable bacteria in urine samples collected from individual animals infected with suspensions of *P. mirabilis* Xen 44 or *P. aeruginosa* Xen 5, with correlation coefficients of 0.95 and 0.88, respectively. No bacteria could be cultured from urine of animals that did not have a bioluminescent signal in the bladder, suggesting that monitoring of infection via bioluminescence is a reasonable measure of bacterial burden. Overall, the percentage of animals with a bladder infection following inoculation with a suspension of *P. mirabilis* Xen 44 remained higher than that with *P. aeruginosa* Xen 5 over the study period (Table 1).

In contrast to those mice inoculated with bacterial suspensions, the bladder signal of mice with catheter-induced infection increased exponentially during the first 24 h after infec-

TABLE 2. Results of bacterial counts in urine after infection[a]

Mode of infection	No. of days after infection	Range of bacterial counts in urine (CFU/ml)		Geometric mean of bacterial counts in urine (CFU/ml)	
		XEN5	XEN44	XEN5	XEN44
Suspension	1	$\leq 1.9 \times 10^2$–1×10^6	N/A$^+$	6.8×10^3	N/A$^+$
	2	$\leq 1.9 \times 10^2$–5×10^5	$\leq 1.9 \times 10^2$–5×10^8	5.7×10^3	3.8×10^5
	6	4.8×10^4–7×10^4	4.8×10^4–1.2×10^8*	1.1×10^3	2.4×10^6*
	9	N/A$^+$	$\leq 1.9 \times 10^2$–2.8×10^8	N/A$^+$	6.4×10^4
	16	$\leq 1.9 \times 10^2$	$\leq 1.9 \times 10^2$–4×10^7	1.9×10^2	6.6×10^4
Postimplant infection	1	$\leq 1.9 \times 10^2$–8×10^7	$\leq 1.9 \times 10^2$–4×10^8	1.3×10^6	4.1×10^7
	2	$\leq 1.9 \times 10^2$–1.4×10^8	$\leq 1.9 \times 10^2$–5×10^8	1.9×10^5	2.9×10^6
	6	N/A$^+$	N/A^{++}	N/A$^+$	N/A^{++}
	9	5×10^5–3×10^6	N/A^{++}	1.2×10^6	N/A^{++}
	16	$\leq 1.9 \times 10^2$–6×10^6	N/A^{++}	2×10^5	N/A^{++}
Precolonized infection	1	$\leq 1.9 \times 10^2$–4×10^6	5×10^6–4.6×10^8	3.3×10^5	4.7×10^7
	2	$\leq 1.9 \times 10^2$–1.8×10^7	8×10^7–1×10^9	7.9×10^5	3×10^8
	6	$\leq 1.9 \times 10^2$–3.3×10^7	1.6×10^8*	1.8×10^5	1.6×10^8*
	9	$\leq 1.9 \times 10^2$–1.7×10^7	N/A^{++}	2.1×10^4	N/A
	16	$\leq 1.9 \times 10^2$–1.4×10^7	N/A^{++}	1.3×10^5	N/A

[a] Symbols: *, number of urine samples less than three due to unsuccessful urine sample collection; N/A$^+$, no data available; N/A^{++}, no data available because animals with infection died.

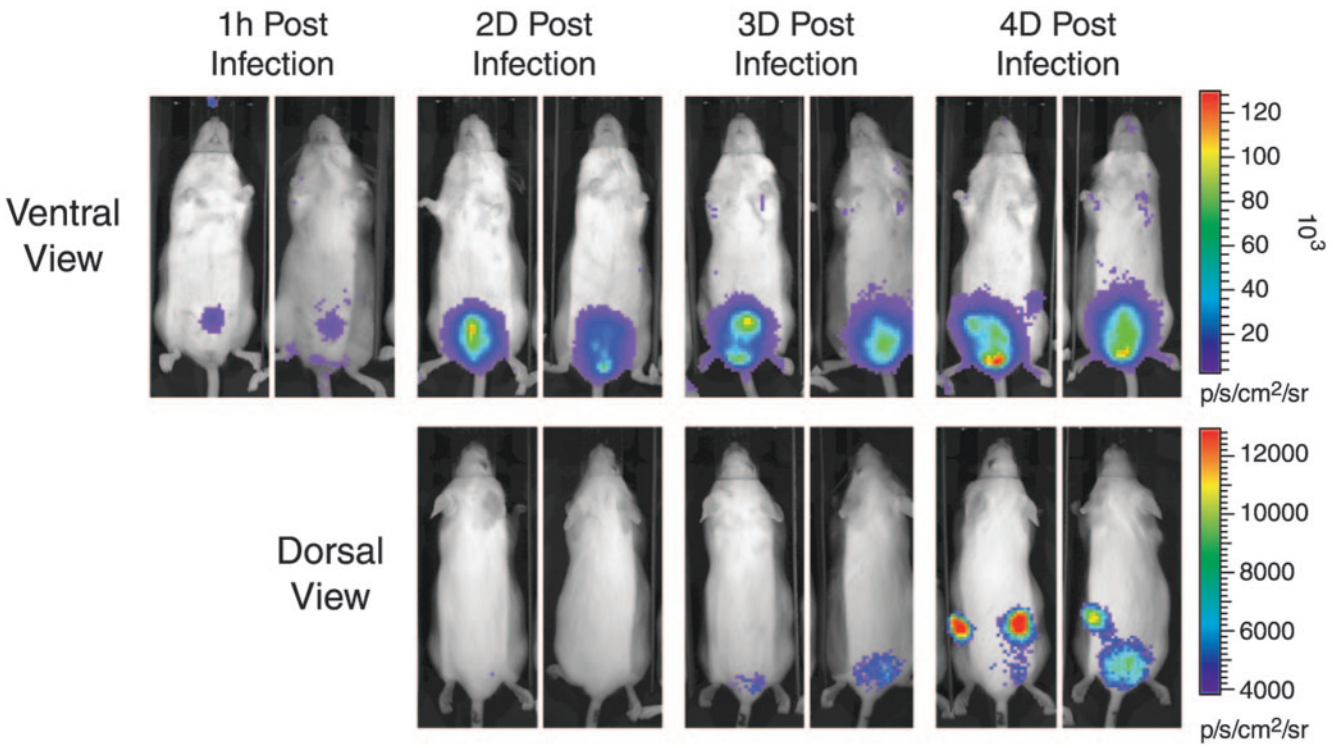

FIG. 2. Monitoring the spread of *P. aeruginosa* Xen 5 infection from the bladder to the kidney by bioluminescence. Mice were infected by placement of a precolonized catheter in the bladder through the urethral meatus, and the infection was monitored by recording photon emission over time. Bacteria ascending from the bladder up the ureters and to the kidney can be clearly visualized (dorsal view) in live animals, using a luciferase tag pathogen and bioluminescence imaging.

tion, reaching ~10^6 to 10^7 photons/s for both *P. aeruginosa* Xen 5 and *P. mirabilis* Xen 44. Catheter-induced infections were not only prolonged but ascended through the ureter to the kidneys (Fig. 2 and Table 1). Persistent infection of the bladder, with the subsequent spontaneous infection of the kidneys, was a feature of foreign body placement in the bladder. The percentage of animals that went on to develop kidney infection tended to be higher with *P. mirabilis* Xen 44 than *P. aeruginosa* Xen 5 (Table 1). Additionally, the bacterial burden required for inducing a coherent infection with *P. mirabilis* Xen 44 (suspension or catheter) was approximately two logs less than that for *P. aeruginosa* Xen 5 (10^4 CFU as oppose to 10^6 CFU). Moreover, all precolonized catheter-infected animals developed cystitis 1 day after infection with *P. mirabilis* Xen 44, and all animals died by day 7. Lowering the inoculum to as low as 10^2 CFU/catheter produced a 54% infection rate in the bladder within a day after placement of the catheter. This suggests that *P. mirabilis* Xen 44 was more virulent in the mouse urinary tract than *P. aeruginosa* Xen 5 (Table 1). The bacterial properties contributing to the difference in infectivity are under investigation. Similar to the bioluminescent signal, the bacterial counts in urine consistently remained elevated over the period of study in catheterized mice, corroborating the bioluminescence data (Table 2). In contrast to those mice inoculated with bacterial suspensions, groups of mice implanted with precolonized catheters maintained a moderately stable bioluminescent signal until termination of the experiment, indicating the chronic nature of foreign body-associated infections.

The progression, morbidity, and persistence of infection produced by different modes of inoculation for both pathogens appeared to be highest when precolonized catheters were used. This was followed by postimplant infection. The lowest levels of progression, persistence, and morbidity for both pathogens were noted in animals infected with a bacterial suspension. This difference in the degree of infection seen between the catheterized and noncatheterized groups clearly indicates the importance of the catheter in potentiation of the infection.

Effect of antimicrobial therapy on *P. mirabilis* Xen 44 infection. To determine whether real-time bioluminescence imaging can be used to evaluate the therapeutic efficacy of antibiotic in real time in the urinary tract, we tested the effect of ciprofloxacin in a group of mice infected with *P. mirabilis* Xen 44. The bioluminescent signal recorded in the bladders of mice challenged with a bacterial suspension or the placement of a precolonized catheter reached approximately 10^7 photons/s 1 day after inoculation. This reasonably intense signal allowed the efficacy of antibiotic treatment to be effectively monitored. The in vivo bioluminescent imaging revealed kidney infection in 39% of *P. mirabilis* Xen 44-catheterized mice after 2 days following inoculation with an average photon flux of 7.8×10^6 photons/s from infected kidneys. The average number of bacteria recovered from kidney homogenates with bioluminescent signal was estimated at 6×10^7 CFU/g kidney. The treatment regimen with ciprofloxacin commenced 2 days after initiation of infection and continued for an additional 4 days. No animals that were left untreated survived beyond 7 days in

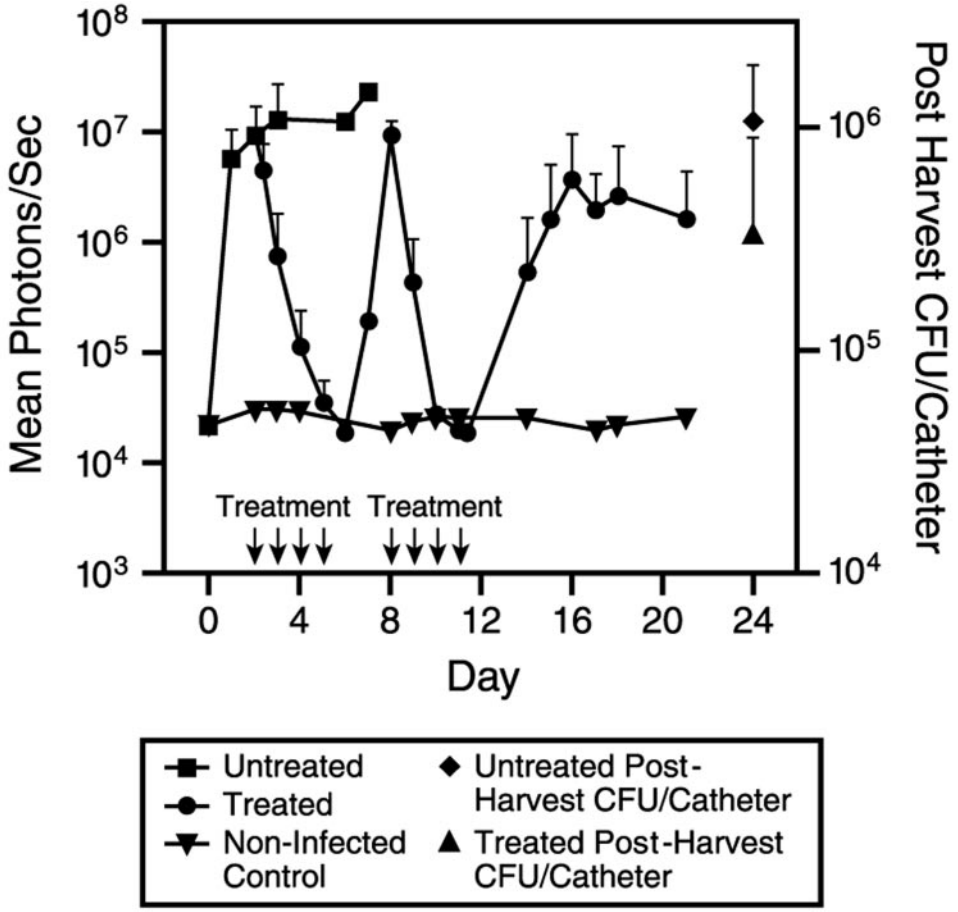

FIG. 3. In vivo bioluminescence monitoring of *P. mirabilis* Xen 44 in the mouse model of UTI during treatment with ciprofloxacin. Effect of ciprofloxacin treatment 2 days after infection and readministration of ciprofloxacin for four additional days after the infection was reestablished. The total number of photons detected per second over the infected bladder was quantified using Living Image software and plotted with respect to time. Each data point is the mean ± standard deviation for 6 to 13 mice. Arrows indicates the days of antibiotic administration. Data are averages of results from three experiments. The viable counts in each catheter were determined immediately after removal from the bladder and are shown in the upper quadrants of the plot.

the group of mice infected by placement of precolonized catheters.

Compared to the untreated control groups, the treated animals inoculated with bacterial suspension showed a rapid decline in bioluminescent signal that was observed by day 1 with an almost 50% reduction and nearly to undetectable levels after 2 days of treatments (data not shown). No bacteria could be cultivated from urine samples of animals that lacked a signal that was above background, suggesting the eradication of infection. A reduction in bioluminescence following treatment in catheterized animals was also observed. However, the decline appeared to be much slower than those seen in animals infected with bacterial suspensions (Fig. 3). Moreover, two additional days of treatments were necessary for the bioluminescent signal to reach background levels. Furthermore, despite completion of a 4-day course of therapy, a weak signal persisted in two of the catheterized animals, demonstrating the difficulty in treating catheter-associated infections. Once reduced, the bioluminescent signal and viable cell numbers remained undetectable for the duration of the study in groups of mice infected with bacterial suspension and treated with ciprofloxacin (data not shown). In contrast, in catheterized mice, the intensity of the residual bioluminescent signal began to increase in 66% of animals approximately 2 days after discontinuing ciprofloxacin treatment, reaching approximately pretreated levels by 8 days postinfection (Fig. 3 and 4), suggesting significant bacterial regrowth in this group of mice. As predicted by the bioluminescent signal, viable bacterial cell numbers also corresponded in urine in these animals. Similar ciprofloxacin data were seen with *P. aeruginosa* Xen 5 infection. However, four additional consecutive days of treatment were required for the bioluminescent signal intensity to reach undetectable levels in catheterized mice (data not shown).

To determine whether the above-described relapses of infection were due to the failure of the antibiotic to completely eradicate the bacteria from the catheter or whether they were due to cells becoming resistant to ciprofloxacin, the antibiotic was readministered for four consecutive days following two days of cessation of initial therapy to mice with reestablished infection (Fig. 3 and 4). Notably, the second attempt to treat the infection again resulted in reduction in bioluminescent signal and the corresponding bacterial count, which was undetectable after 3 days of ciprofloxacin treatment. This demon-

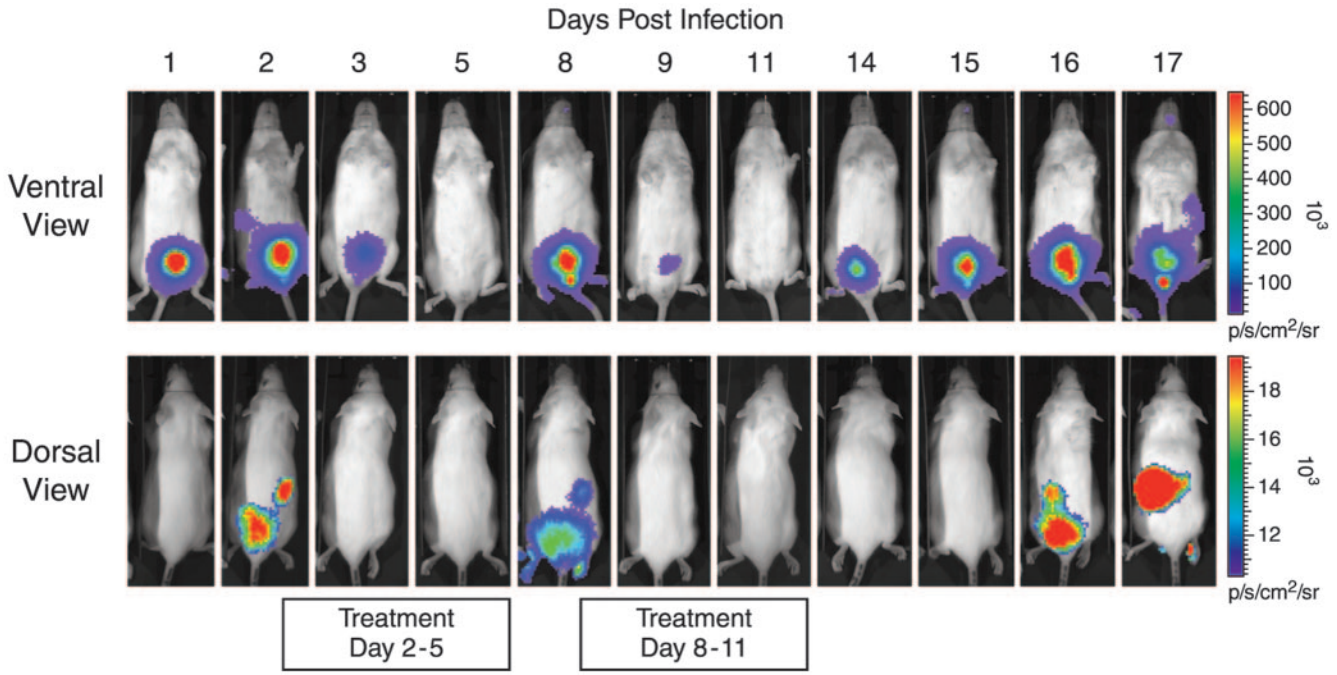

FIG. 4. Real-time monitoring of the effects of ciprofloxacin on *P. mirabilis* Xen 44 UTI. A representative animal from the group receiving antibiotic is shown. Note that the response to treatment, including relapse and renal infection, can be monitored noninvasively within the same animal throughout the study period.

strated that bacterial regrowth was not a result of the cells becoming resistant to the antibiotic but more likely was due to a small proportion of the cells surviving and dividing once the antibiotic was no longer present. Indeed, bacteria recovered from catheters from mice with recurring infection following ciprofloxacin treatment were confirmed to be sensitive to the antibiotic by MIC. The bioluminescent signal in animals with kidney infections also declined with therapy and returned to background levels after 4 days of treatment (Fig. 4). No bacteria could be cultivated from kidney homogenates of these animals at the time of sacrifice, indicating that bioluminescence is a convenient method of monitoring infection and response to treatment. Interestingly, after the second treatment, the signals in the bladder and kidney rebounded again, this time in 50% of animals, and reached levels seen in those of pretreated mice. Paralleling the bioluminescence data, the bacterial counts in urine also started to increase after cessation of ciprofloxacin treatment (Fig. 4). Compared to real-time bioluminescence monitoring, conventional methods for estimating the number of viable bacteria present in vivo and the efficacy of drug treatment were considerably longer.

Electron microscopy of catheter from mouse bladder. Scanning electron microscopic examination of catheters harvested from the mouse bladders after 2 days demonstrated that the lumen and the surface of the catheter were covered with thick biofilm and rod-shaped bacterial cells mostly buried within the matrix (Fig. 5). This encrustation may have protected the bacteria from antibiotic killing and thus caused persistent or recurrent infections. It also demonstrated that the implanted device constitutes a particularly attractive surface for bacterial colonization and biofilm development in vivo.

DISCUSSION

In the present study, we have demonstrated the application of biophotonic imaging to monitor catheter-associated UTI in living mice. Two common human uropathogens, *P. aeruginosa* and *P. mirabilis*, were made bioluminescent by the insertion of a complete *lux* operon into their chromosomes, and these engineered strains were used to study the infection process in real time from outside of the infected animals, using a low-light optical imaging system. We adapted the rat model of foreign body-associated UTI developed by Kurosaka et al. (26) to demonstrate that placement of a foreign body in the bladder of a mouse without surgical manipulation allows establishment of a reproducible persistent chronic infection. We also demonstrated the use of this model to study the therapeutic response of these uropathogens to ciprofloxacin, a commonly used antibiotic in treatment of UTI. We were able to visualize the entire course of the infection, including subsequent disease relapse, which was seen to occur following termination of treatment in animals with catheters implanted. This procedure ensured that a minimal number of animals were used and that little manipulation of the urinary tract was necessary. In this respect, our model is comparable to the clinical situation, in which relapse and the recalcitrant nature of the infection even with treatment are commonly seen. The phenomenon probably contributes significantly to the frequent failures of antibiotic therapy on biofilm infections in humans. An important and unique aspect of the present study was the capacity to monitor ascending UTI in catheter-associated infections, demonstrating this murine model to closely resemble the natural human condition that frequently leads to pyelonephritis.

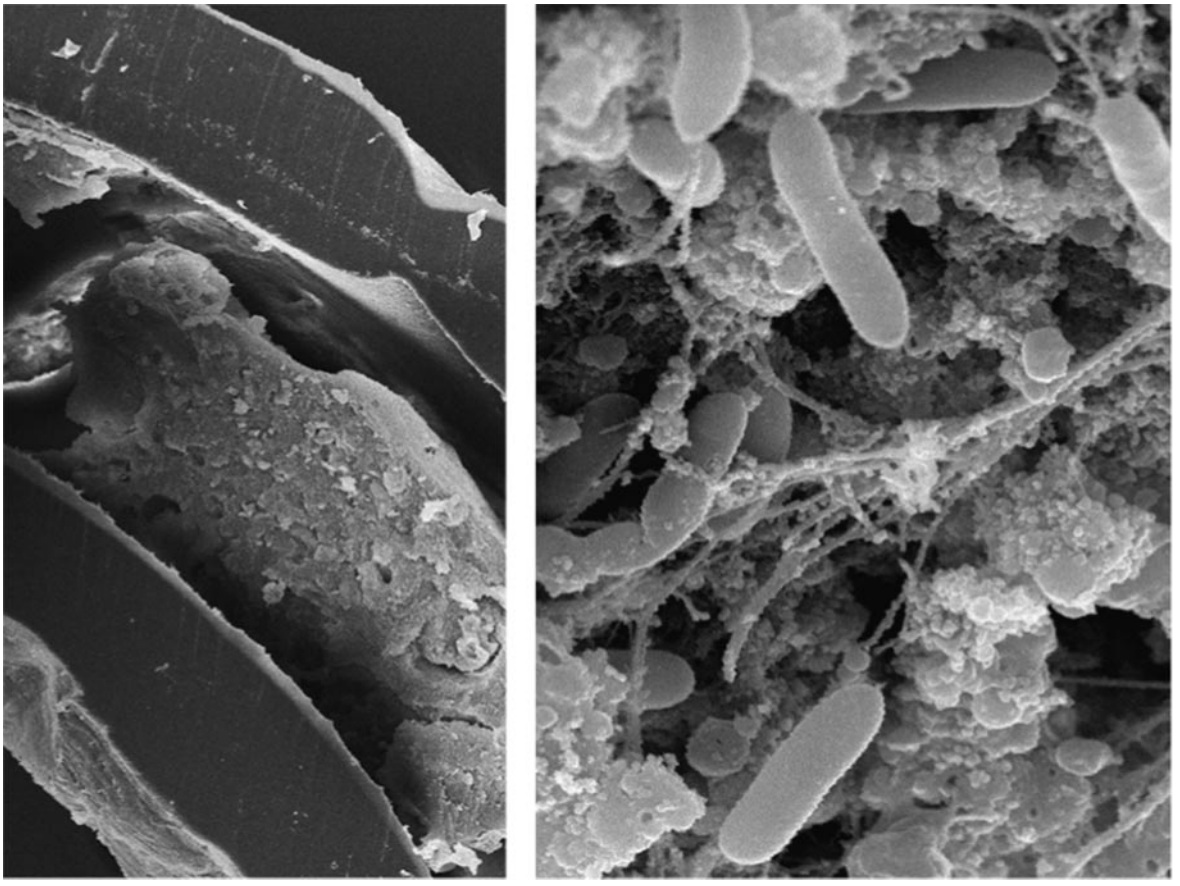

FIG. 5. Scanning electron micrograph of a longitudinal section of a catheter from the bladder of a mouse 2 days after infection. Cross-section of catheter at low magnification (left) shows the lumen of the catheter filled with a thick biofilm. Also note a thin film outside the surface of the catheter. Numerous rod-shaped bacterial cells mostly embedded within the intracellular material are clearly seen at higher magnification (right).

Another feature of the present study was the capacity to mimic the clinical situation of intraoperative or postoperative contamination. We examined this by either implanting a precoated catheter with a defined inoculum of bacteria or by infecting the bladder with a defined inoculum of bacteria after placing a sterile catheter in the bladder. Both approaches are clinically relevant and we found that the infection rate was highest when implanting a precolonized catheter followed by postimplant infection. The lowest incidence of morbidity and mortality was recorded after inoculation of bacterial suspension in the absence of a foreign body in the bladder. The model is therefore useful for studying foreign body-associated infections and pathologies within the urinary tract. Interestingly, *P. mirabilis* Xen 44 was shown to have a high virulence even at doses as low as 10^2 CFU per catheter in this model. Despite this high morbidity and mortality, we were able to establish a chronic infection in catheterized mice by administering antibiotic treatment to the animals at an early stage of infection. This way, we were able to monitor the disease in catheterized mice until the termination of the study on day 21.

Urinary tract infections induced with bacterial suspensions were shown to respond rapidly to ciprofloxacin and were efficiently eradicated by this therapy. In contrast, despite planktonic *P. mirabilis* Xen 44 and *P. aeruginosa* Xen 5 sensitivity to ciprofloxacin, both pathogens induced a persistent and recurrent infection following treatment in catheterized animals, demonstrating the difficulty associated with resolving biofilm infections on implanted bodies. Microscopically, both pathogens were seen to grow as a biofilm on the inside and the outside of the catheter, and it is likely that this mode of growth in some way impeded the effectiveness of the drug, although the exact mechanism behind this impedance was not identified. The therapeutic efficacy of ciprofloxacin against UTI including foreign body-associated UTI caused by several uropathogens has been shown previously (13, 39, 46). Our results are consistent with previous observations. However, the relapse of infection in catheterized mice following cessation of treatment shown in the present study has not been reported in studies conducted with conventional ex vivo methods (39). These methods require the sacrificing of animals for sampling and therefore will not permit longitudinal monitoring of infection in the same animal. This indeed may have prevented the detection of regrowth of bacteria in foreign body-associated UTI following the termination of ciprofloxacin treatment. This highlights the importance of monitoring therapeutic efficacies and relapse of infection in the same animal following the termination of treatment regimens. By the method described here, it was possible to evaluate regrowth of bacteria without the limitations associated with death as an end point for sampling.

Relapse of infection following treatment, a condition frequently seen with catheterized animals during this study and in similar studies conducted previously using optical imaging (21, 22, 45), resembles the clinical conditions. In this respect, our model is well suited for evaluating antibacterial activity with chronic biofilm infections in the urinary tract. A plausible explanation for relapse is that although the antibiotic was able to kill planktonic swarmer cells shed into the urine from the catheter surface, a small proportion of the bacteria within the biofilm were protected and survived killing by the antibiotic treatment, only to subsequently proliferate and produce new swarmer cells that went on to cause a recurrence of the infection. Why a small proportion of these cells should survive the antibiotic therapy is not known (growth phase or location in the biofilm matrix); however, antibiotics frequently work in combination with the host's immune system, and it is possible that the physical barrier generated by the biofilm acts to inhibit immune cells from effectively penetrating and eradicating straggling bacterial cells that are not immediately killed by the ciprofloxacin. Our bioluminescence data support such an interpretation of events in catheterized mice, since with each treatment there was a dramatic decline in the luminescent signal from the bladder of these animals and a corresponding reduction in the number of viable bacteria in urine, followed by a staggered rebound of this signal over time.

In a few cases the bioluminescent signal persisted longer on the catheters in some animals even after ciprofloxacin treatment. We were able to confirm that the signal was indeed emanating from catheter by ex vivo imaging of harvested catheters after these animals had completed 3 days of treatment. Furthermore, we were able to culture viable bacteria from these catheters. We also noticed a high incidence of renal infections and mortality in mice with catheter-induced (precolonized or postimplant) infection. This frequency of morbidity and mortality appeared to be even greater with *P. mirabilis* Xen 44. Kurosaka et al. (26) observed similar results with *P. aeruginosa* foreign body-associated urinary tract infection in rats and proposed that the biofilms on the catheters acted as a reservoir for the bacteria, constantly releasing cells into the bladder, thereby allowing the ascending infection into the kidneys throughout the experimental period. Another possibility is that the bacteria are able to invade the bladder epithelium and subsequently grow to form a mature biofilm, as shown for *E. coli* (1, 36). Unlike free-floating pathogens, those bacteria within the bladder mucosa are known to reemerge and eventually establish a persistent, dormant bacterial reservoir that may serve as a source for recurrent infections. However, our electron microscopic examination of the bladder surface did not show pod-like structures as shown for *E. coli*.

Several models of UTIs have been described (14, 18, 19, 26, 27, 34, 37, 41, 49). A number of these studies were conducted to investigate the pathogenesis of various uropathogens and for the evaluation of different antibiotics for UTIs in laboratory animals (2, 8, 11, 12, 17, 23, 33, 39, 40, 43, 46). However, monitoring the infections in these animal models using conventional methods is cumbersome, laborious, and time consuming. Conventional methods estimate the pathogen burden by estimating the numbers of recovered CFU from organs and urine samples. Monitoring the infection based on bacteriuria has been shown to be inconsistent in confirming the true infection in the bladder or kidney (14, 16, 17). Because the distal urethra is normally colonized with large numbers of different bacterial species, the diagnosis of clinically significant bacteriuria is difficult. In this respect our approach is attractive, because our bioluminescent bacteria can be easily distinguished from contaminating bacteria in the urethral meatus. Moreover, using conventional methods it is crucial to sacrifice animals and excise tissues to determine progression of the infection, pathogenesis, or therapeutic efficacy.

Antibiotic efficacy is determined in conventional studies by looking for a reduction in the pathogen burden during sampling or by counting the number of surviving animals following treatment. Such methods require large numbers of animals, lengthy incubation periods, and removal and processing of tissue to locate and quantify the infecting pathogen. A major drawback with these ex vivo methods is the difficulty in extracting the bacteria, animal-to-animal variations in experimental data, problems of antibiotic carry-over, phenotypic conversion from sessile to planktonic, and performance of the experiment in the absence of animal host defense mechanisms. Using optical imaging, we were able to overcome these limitations by visualizing the disease process from outside intact infected animals. With this simple, nonintrusive technique, we were able to streamline and refine a foreign body-associated urinary tract infection in a mouse model, allowing repeated imaging of the same animal over time to provide more information per animal while using significantly fewer animals overall.

ACKNOWLEDGMENT

We thank C. Dalesio (Graphics and Communications, Xenogen Corporation) for assistance with drawings.

REFERENCES

1. **Anderson, G. G., J. J. Palermo, J. D. Schilling, R. Roth, J. Heuser, and S. J. Hultgren.** 2003. Intracellular bacterial biofilm-like pods in urinary tract infections. Science **301:**105–107.
2. **Berry, V., R. Page, J. Satterfield, C. Singley, R. Straub, and G. Woodnutt.** 2000. Comparative efficacy of gemifloxacin in experimental models of pyelonephritis and wound infection. J. Antimicrob. Chemother. **45**(Suppl. 1)**:** 87–93.
3. **Contag, C. H., P. R. Contag, J. I. Mullins, S. D. Spilman, D. K. Stevenson, and D. A. Benaron.** 1995. Photonic detection of bacterial pathogens in living hosts. Mol. Microbiol. **18:**593–603.
4. **Contag, P. R., I. N. Olomu, D. K. Stevenson, and C. H. Contag.** 1998. Bioluminescent indicators in living mammals. Nat. Med. **4:**245–247.
5. **Davies, D.** 2003. Understanding biofilm resistance to antibacterial agents. Nat. Rev. Drug Discov. **2:**114–122.
6. **Dickinson, G. M., and A. L. Bisno.** 1989. Infections associated with indwelling devices: infections related to extravascular devices. Antimicrob. Agents Chemother. **33:**602–607.
7. **Doyle, T. C., S. M. Burns, and C. H. Contag.** 2004. *In vivo* bioluminescence imaging for integrated studies of infection. Cell Microbiol. **6:**303–317.
8. **Fernandes, P. B., C. W. Hanson, J. M. Stamm, C. Vojtko, N. L. Shipkowitz, and E. St Martin.** 1987. The frequency of in-vitro resistance development to fluoroquinolones and the use of a murine pyelonephritis model to demonstrate selection of resistance *in vivo*. J. Antimicrob. Chemother. **19:**449–465.
9. **Foxman, B.** 2003. Epidemiology of urinary tract infections: incidence, morbidity, and economic costs. Dis. Mon. **49:**53–70.
10. **Francis, K. P., J. Yu, C. Bellinger-Kawahara, D. Joh, M. J. Hawkinson, G. Xiao, T. F. Purchio, M. G. Caparon, M. Lipsitch, and P. R. Contag.** 2001. Visualizing pneumococcal infections in the lungs of live mice using bioluminescent *Streptococcus pneumoniae* transformed with a novel gram-positive *lux* transposon. Infect. Immun. **69:**3350–3358.
11. **Frosco, M. B., J. L. Melton, F. P. Stewart, B. A. Kulwich, L. Licata, and J. F. Barrett.** 1996. *In vivo* efficacies of levofloxacin and ciprofloxacin in acute murine hematogenous pyelonephritis induced by methicillin-susceptible and -resistant *Staphylococcus aureus* strains. Antimicrob. Agents Chemother. **40:** 2529–2534.
12. **Fu, K. P., S. C. Lafredo, B. Foleno, D. M. Isaacson, J. F. Barrett, A. J. Tobia, and M. E. Rosenthale.** 1992. *In vitro* and *in vivo* antibacterial activities of

levofloxacin (l-ofloxacin), an optically active ofloxacin. Antimicrob. Agents Chemother. **36:**860–866.
13. **Fukuoka, Y., Y. Ikeda, Y. Yamashiro, M. Takahata, Y. Todo, and H. Narita.** 1993. *In vitro* and *in vivo* antibacterial activities of T-3761, a new quinolone derivative. Antimicrob. Agents Chemother. **37:**384–392.
14. **Hagberg, L., I. Engberg, R. Freter, J. Lam, S. Olling, and C. Svanborg Eden.** 1983. Ascending, unobstructed urinary tract infection in mice caused by pyelonephritogenic *Escherichia coli* of human origin. Infect. Immun. **40:**273–283.
15. **Hardy, J., K. P. Francis, M. DeBoer, P. Chu, K. Gibbs, and C. H. Contag.** 2004. Extracellular replication of *Listeria monocytogenes* in the murine gall bladder. Science **303:**851–853.
16. **Hultgren, S. J., T. N. Porter, A. J. Schaeffer, and J. L. Duncan.** 1985. Role of type 1 pili and effects of phase variation on lower urinary tract infections produced by *Escherichia coli*. Infect. Immun. **50:**370–377.
17. **Hvidberg, H., C. Struve, K. A. Krogfelt, N. Christensen, S. N. Rasmussen, and N. Frimodt-Moller.** 2000. Development of a long-term ascending urinary tract infection mouse model for antibiotic treatment studies. Antimicrob. Agents Chemother. **44:**156–163.
18. **Johnson, D. E., C. V. Lockatell, M. Hall-Craggs, and J. W. Warren.** 1991. Mouse models of short- and long-term foreign body in the urinary bladder: analogies to the bladder segment of urinary catheters. Lab. Anim. Sci. **41:** 451–455.
19. **Jones, B. D., C. V. Lockatell, D. E. Johnson, J. W. Warren, and H. L. Mobley.** 1990. Construction of a urease-negative mutant of *Proteus mirabilis:* analysis of virulence in a mouse model of ascending urinary tract infection. Infect. Immun. **58:**1120–1123.
20. **Kadurugamuwa, J. L., L. Sin, E. Albert, J. Yu, K. Francis, M. DeBoer, M. Rubin, C. Bellinger-Kawahara, T. R. Parr Jr., and P. R. Contag.** 2003. Direct continuous method for monitoring biofilm infection in a mouse model. Infect. Immun. **71:**882–890.
21. **Kadurugamuwa, J. L., L. V. Sin, J. Yu, K. P. Francis, R. Kimura, T. Purchio, and P. R. Contag.** 2003. Rapid direct method for monitoring antibiotics in a mouse model of bacterial biofilm infection. Antimicrob. Agents Chemother. **47:**3130–3137.
22. **Kadurugamuwa, J. L., L. V. Sin, J. Yu, K. P. Francis, T. F. Purchio, and P. R. Contag.** 2004. Noninvasive optical imaging method to evaluate postantibiotic effects on biofilm infection in vivo. Antimicrob/ Agents Chemother. **48:** 2283–2287.
23. **Kerrn, M. B., N. Frimodt-Moller, and F. Espersen.** 2003. Effects of sulfamethizole and amdinocillin against *Escherichia coli* strains (with various susceptibilities) in an ascending urinary tract infection mouse model. Antimicrob. Agents Chemother. **47:**1002–1009.
24. **Kuklin, N. A., G. D. Pancari, T. W. Tobery, L. Cope, J. Jackson, C. Gill, K. Overbye, K. P. Francis, J. Yu, D. Montgomery, A. S. Anderson, W. McClements, and K. U. Jansen.** 2003. Real-time monitoring of bacterial infection in vivo: development of bioluminescent staphylococcal foreign-body and deep-thigh-wound mouse infection models. Antimicrob. Agents Chemother. **47:**2740–2748.
25. **Kumon, H.** 2000. Management of biofilm infections in the urinary tract. World J. Surg. **24:**1193–1196.
26. **Kurosaka, Y., Y. Ishida, E. Yamamura, H. Takase, T. Otani, and H. Kumon.** 2001. A non-surgical rat model of foreign body-associated urinary tract infection with *Pseudomonas aeruginosa*. Microbiol. Immunol. **45:**9–15.
27. **Lecamwasam, J. P., and T. E. Miller.** 1989. Antimicrobial agents in the management of urinary tract infection: an experimental evaluation. J. Lab. Clin. Med. **114:**510–519.
28. **Lemos, B., L. Sin, J. Yu, K. P. Francis, and J. L. Kadurugamuwa.** 2004. Rapid method to monitor catheter-based urinary tract infection in mice using biophotonic imaging. Abstr. 104th Gen. Meet. Am. Soc. Microbiol., abstr. D-117. American Society for Microbiology, Washington, D.C.
29. **Lewis, K.** 2001. Riddle of biofilm resistance. Antimicrob. Agents Chemother. **45:**999–1007.
30. **Luker, G. D., J. L. Prior, J. Song, C. M. Pica, and D. A. Leib.** 2003. Bioluminescence imaging reveals systemic dissemination of herpes simplex virus type 1 in the absence of interferon receptors. J. Virol. **77:**11082–11093.
31. **Marrie, T. J., and J. W. Costerton.** 1984. Scanning and transmission electron microscopy of in situ bacterial colonization of intravenous and intraarterial catheters. J. Clin. Microbiol. **19:**687–693.
32. **Mermel, L. A., B. M. Farr, R. J. Sherertz, I. I. Raad, N. O'Grady, J. S. Harris, and D. E. Craven.** 2001. Guidelines for the management of intravascular catheter-related infections. Clin. Infect. Dis. **32:**1249–1272.
33. **Meulbroek, J. A., A. Oleksijew, S. K. Tanaka, and J. D. Alder.** 1996. Efficacy of ABT-719, a 2-pyridone antimicrobial, against enterococci, *Escherichia coli*, and *Pseudomonas aeruginosa* in experimental murine pyelonephritis. J. Antimicrob. Chemother. **38:**641–653.
34. **Mobley, H. L., and J. W. Warren.** 1987. Urease-positive bacteriuria and obstruction of long-term urinary catheters. J. Clin. Microbiol. **25:**2216–2217.
35. **Morris, N. S., D. J. Stickler, and R. J. McLean.** 1999. The development of bacterial biofilms on indwelling urethral catheters. World J. Urol. **17:**345–350.
36. **Mulvey, M. A., J. D. Schilling, and S. J. Hultgren.** 2001. Establishment of a persistent *Escherichia coli* reservoir during the acute phase of a bladder infection. Infect. Immun. **69:**4572–4579.
37. **Nishi, T., and K. Tsuchiya.** 1978. Experimental urinary tract infection with *Pseudomonas aeruginosa* in mice. Infect. Immun. **22:**508–515.
38. **Nishino, T., and Y. Obana.** 1996. Therapeutic efficacy of intravenous and oral ciprofloxacin in experimental murine infections. Chemotherapy **42:**140–145.
39. **Otani, T., M. Tanaka, E. Ito, Y. Kurosaka, Y. Murakami, K. Onodera, T. Akasaka, and K. Sato.** 2003. In vitro and in vivo antibacterial activities of DK-507k, a novel fluoroquinolone. Antimicrob. Agents Chemother. **47:** 3750–3759.
40. **Ozaki, M., M. Matsuda, Y. Tomii, K. Kimura, J. Segawa, M. Kitano, M. Kise, K. Shibata, M. Otsuki, and T. Nishino.** 1991. In vivo evaluation of NM441, a new thiazeto-quinoline derivative. Antimicrob. Agents Chemother. **35:**2496–2499.
41. **Satoh, M., K. Munakata, K. Kitoh, H. Takeuchi, and O. Yoshida.** 1984. A newly designed model for infection-induced bladder stone formation in the rat. J. Urol. **132:**1247–1249.
42. **Sin, L., B. Lemos, J. Yu, K. P. Francis, A. S. Bayer, Y. Xiong, and J. L. Kadurugamuwa.** 2004. A direct method for real-time monitoring of establishment and progression of *in vivo* infections on intravascular catheters. Abstr. 104th Gen. Meet. Am. Soc. Microbiol., abstr. B-437. American Society for Microbiology, Washington, D.C.
43. **Tomii, Y., M. Ozaki, M. Matsuda, T. Honmura, I. Nishimura, R. Yamaguchi, T. Adachi, Y. Okawa, and T. Nishino.** 1996. Therapeutic effect of the quinolone prodrug prulifloxacin against experimental urinary tract infections in mice. Arzneimittelforschung **46:**1169–1173.
44. **Warren, J. W.** 1997. Catheter-associated urinary tract infections. Infect. Dis. Clin. N. Am. **11:**609–622.
45. **Xiong, Y. Q., J. Willard, J. L. Kadurugamuwa, J. Yu, K. P. Francis, and A. S. Bayer.** 2004. Real-Time in vivo bioluminescent imaging for evaluating the efficacy of antibiotics in a rat *Staphylococcus aureus* endocarditis model. Antimicrob. Agents Chemother. **49:**380–397.
46. **Yoshizumi, S., Y. Takahashi, M. Murata, H. Domon, N. Furuya, Y. Ishii, T. Matsumoto, A. Ohno, K. Tateda, S. Miyazaki, and K. Yamaguchi.** 2001. The *in vivo* activity of olamufloxacin (HSR-903) in systemic and urinary tract infections in mice. J. Antimicrob. Chemother. **48:**137–140.
47. **Yu, Y. A., S. Shabahang, T. M. Timiryasova, Q. Zhang, R. Beltz, I. Gentschev, W. Goebel, and A. A. Szalay.** 2004. Visualization of tumors and metastases in live animals with bacteria and vaccinia virus encoding light-emitting proteins. Nat. Biotechnol. **22:**313–320.
48. **Zhao, M., M. Yang, E. Baranov, X. Wang, S. Penman, A. R. Moossa, and R. M. Hoffman.** 2001. Spatial-temporal imaging of bacterial infection and antibiotic response in intact animals. Proc. Natl. Acad. Sci. USA **98:**9814–9818.
49. **Zunino, P., L. Geymonat, A. G. Allen, C. Legnani-Fajardo, and D. J. Maskell.** 2000. Virulence of a Proteus mirabilis ATF isogenic mutant is not impaired in a mouse model of ascending urinary tract infection. FEMS Immunol. Med. Microbiol. **29:**137–143.

Editor: A. D. O'Brien